Revista Mexicana de Ciencias Forestales Vol. 16 (89)
Mayo - Junio (2025)

DOI: 10.29298/rmcf.v16i89.1542

Research Article

Estimación de la biomasa forestal aérea a nivel árbol individual mediante LiDAR terrestre

Aboveground forest biomass estimation at the individual tree level using terrestrial LiDAR

Jorge Luis Compeán-Aguirre[1], Pablito Marcelo López-Serrano[2]*, José Luís Silván-Cárdenas[3], Ciro Andrés Martínez-García-Moreno[4], Daniel José Vega-Nieva[5], José Javier Corral-Rivas[5]

Fecha de recepción/Reception date: 14 de diciembre de 2024.
Fecha de aceptación/Acceptance date: 28 de marzo de 2025.

[1]Universidad Juárez del Estado de Durango, Programa Institucional de Doctorado en Ciencias Agropecuarias y Forestales. México.
[2]Universidad Juárez del Estado de Durango, Instituto de Silvicultura de la Industria de la Madera. México.
[3]Centro de Investigación en Ciencias de Información Geoespacial. México.
[4]Instituto Politécnico Nacional, Centro de Investigación y Desarrollo de Tecnología Digital. México.
[5]Universidad Juárez del Estado de Durango, Facultad de Ciencias Forestales. México.

*Autor para correspondencia; correo-e: p_lopez@ujed.mx
*Corresponding author; e-mail: p_lopez@ujed.mx

Abstract

Forest ecosystems play a key role in carbon storage, highlighting the importance of accurately estimating the tree biomass. The objective was to estimate the forest biomass using a laser scanner (LiDAR, Light Detection and Ranging), specifically a terrestrial device (TLS, Terrestrial Laser Scanner), at the individual tree level. Thirty-one trees were selected from a *Pinus cooperi* regular stand, whose diameter at breast height (*DBH*) and height (*h*) variables were measured in a traditional way. TLS data were collected with a model Focus M70 FARO® laser scanner and processed to three-dimensionally model the logs and calculate their biomass. These data were compared with estimates obtained by allometric equations and traditional measurements. Results indicate that the TLS is accurate in measuring diameters (R^2=0.72 and *RMSE*=1.28 cm), compared to traditional methods. However, it underestimates the tree height (R^2=0.79 and *RMSE*=1.68 m), affecting the accuracy of the biomass calculation. Although the TLS provided acceptable estimates, these were lower than those obtained using allometric equations. In conclusion, TLS is a promising tool for nondestructive biomass studies. Future work should consider in greater detail the influence of the characteristics of the studied area, the scanning methodology, and the algorithms applied in the estimation of biomass.

Key words: Circumference adjustment, biomass, terrestrial laser scanning, 3D modeling, point cloud, forest parameters.

Resumen

Los ecosistemas forestales desempeñan un papel clave en el almacenamiento de carbono, lo que subraya la importancia de estimar la biomasa de los árboles de manera precisa. El objetivo de la presente investigación fue estimar la biomasa forestal mediante un escáner láser (*LiDAR*, por sus siglas en inglés *Light Detection and Ranging*), específicamente un dispositivo terrestre (*TLS*, *Terrestrial Laser Scanner*), a nivel de árbol individual. Se seleccionaron 31 árboles de una masa regular de *Pinus cooperi* de los cuales se midieron las variables de diámetro a la altura del pecho (*DAP*) y la altura (*h*), de manera tradicional. Los datos de *TLS* se recolectaron con un escáner laser *FARO*® Focus M70, se procesaron para modelar tridimensionalmente los troncos y calcular su biomasa. Estos datos se contrastaron con estimaciones obtenidas por ecuaciones alométricas y mediciones tradicionales. Los resultados indican que el *TLS* es preciso para medir diámetros (R^2=0.72 y *RMSE*=1.28 cm), respecto a los métodos tradicionales. Sin embargo, subestima la altura de los árboles (R^2=0.79 y *RMSE*=1.68 m), lo que afecta la precisión en el cálculo de la biomasa. Aunque el *TLS* proporcionó estimaciones aceptables, estas fueron inferiores a las obtenidas mediante ecuaciones alométricas. Se concluye que el *TLS* es una herramienta prometedora para estudios no destructivos de biomasa. Futuros trabajos deben considerar con mayor detalle la influencia de las características del área estudiada, la metodología del escaneo y los algoritmos aplicados en la estimación de la biomasa.

Palabras clave: Ajuste de circunferencia, biomasa, escaneo láser terrestre, modelado 3D, nube de puntos, parámetros forestales.

Introduction

Forest ecosystems are the main reservoir of aerial biomass. During photosynthesis, they capture carbon dioxide and release oxygen. Subsequently, the carbon fixed in their tissues is transferred to the soil through the decomposition of organic matter. For this reason, the accurate estimation of biomass makes it possible to quantify the carbon storage capacity of forests. Traditionally, methodologies based on destructive sampling have been used to develop allometric models to estimate aboveground biomass (Segura & Andrade, 2008). The most commonly used models include linear, nonlinear, and mixed-effects regression derivatives (Návar, 2009; Vargas-Larreta et al., 2017).

The main independent variables considered in these equations are diameter at breast height (*DBH*), *i. e.*, at 1.30 m from the ground, and total height, both of which are easy to measure (Huy et al., 2016). However, these expressions are often specific to certain geographic regions or species, a fact that limits their applicability in areas where local data are not available (Chojnacky et al., 2014). In addition, the collected data must comply with certain statistical assumptions for their correct application, such as independence of the data, normal distribution, and constant variance, as well as assuming a minimum error in the measurement of the independent variables (Ashraf et al., 2013).

Within this context, new methodologies based on remote sensing technologies applied to forest measurement, such as LiDAR devices, have emerged. The main platforms for these devices are: the spatial such as NASA's ICESat-2 and GEDI, Airborne Laser Scanning (ALS), and the Terrestrial Laser Scanning (TLS), which includes Mobile Laser Scanning (MLS) and Personal Laser Scanning (PLS) (Borsah et al., 2023). LiDAR systems work by emitting laser pulses that, when interacting with a surface, reflect part of the energy back to the sensor; the process generates three-dimensional data of the scanned entities, making it possible to obtain, with high accuracy, a three-dimensional model of the objects (Disney et al., 2018).

Each LiDAR platform has specific characteristics. TLS offers high accuracy in the three-dimensional reconstruction of individual trees, but its range is limited, and it captures the forest canopy poorly due to branch occlusion. ALS covers large forest areas with high resolution, although its accuracy depends on laser penetration into the vegetation. MLS provides continuous scanning and covers large areas in less time than TLS, but its accuracy can be affected by positioning errors and inherent motion noise. Finally, space LiDAR provides global monitoring of forest biomass but has a lower resolution and is subject to satellite orbital coverage (Borsah et al., 2023).

The estimation of forest aboveground biomass using TLS can be divided into two main approaches: structural modeling (Calders et al., 2015), and extraction of dendrometric parameters (Kankare et al., 2013). Recently, satellite images and artificial intelligence algorithms have been integrated to the TLS data, among which the use of neural networks stands out for its greater precision in biomass estimation (Bhandari & Nandy, 2024; Wang et al., 2023). Globally, China and the United States of America are leading in the application of TLS for biomass calculation, especially in temperate forests (Compeán-Aguirre & López-Serrano, 2024).

In Mexico, the use of TLS is still limited. Previous forest research has documented the development of the TreeTool v0.1 program, which can measure *DBH* and height in ALS and TLS data (Montoya et al., 2021), the application of a MLS to measure forest inventory parameters (Hernández-Moreno et al., 2025a), and the calculation of volume and biomass (Hernández-Moreno et al., 2025b). On the other hand, airborne LiDAR has been more studied, with several researches focused on forest inventories and aerial biomass estimates (Galeote-Leyva et al., 2022; Islas-Gutiérrez et al., 2024; Ortiz-Reyes et al., 2019, 2022). Despite the conducted research, technical and methodological challenges remain, highlighting the need to study the terrestrial LiDAR at the national level.

Based on the above, the objective of this study was to estimate forest biomass at the individual tree level using data from a Terrestrial LiDAR sensor (TLS). For this purpose, the total height and diameter variables were extracted and used to model the stem of each tree. The results were compared with estimates derived from allometric equations.

Materials and Methods

Study area

The study was conducted in a site with a regular forest stand of *Pinus cooperi* C. E. Blanco, with a dimension of 50×50 meters and a density of 960 trees ha^{-1}, located in the *La Victoria ejido*, *Pueblo Nuevo* municipality, state of *Durango*, Mexico (Figure 1A). The site was established under the methodology developed by the Forest Commission (Hummel et al., 1959). Here, homogeneous areas are divided into plots that can range between 1 200 and 4 000 m^2, where trees are numbered and periodically measured to monitor their growth. The study area has a temperate sub-humid and semi-cold sub-humid climate (García, 2004), with an average annual temperature of 20 to 22 °C and annual precipitation between 800 to 1 200 mm.

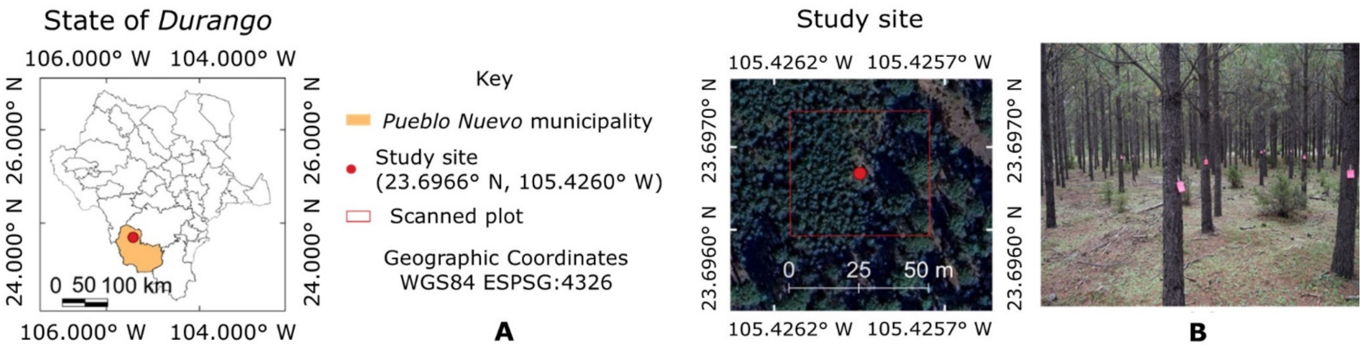

A = Geographical location of the study area; B = Selected and labeled site trees.

Figure 1. Study area.

Data collection

Thirty-one trees with a *DBH* of over 10 cm (Hoover & Smith, 2020) were randomly selected and marked with pink labels for identification in the TLS point cloud (Figure

1B). The *DBH* of each tree was measured at 1.30 m above the ground with a model Mantax Blue Häglof® 800 mm forest caliper, and two perpendicular measurements with a North-South and East-West orientation were averaged. The height (*h*) of each individual was obtained with a model Vertex 5 Haglöf® hypsometer.

Once the direct measurements were taken, a laser scanning was performed. The location of the sensor and the distribution of the trees are key to not losing information; therefore, it is recommended to carry out multiple scans (Liang et al., 2018). Four positions were determined to cover most of the trees, with an average of 9 minutes per scan, based on the work of Bornand et al. (2023), who used three scans in a temperate forest. The positions where the equipment was placed and the distribution of the trees are shown in Figure 2A. The device used was a model Focus M70 FARO® scanner; with a wavelength of 1 550 nm, a measuring range of 0.6 to 70 m, and an accuracy of ±3 mm; it records a laser pulse reflection and captures RGB images of up to 165 megapixels. The setup profile was "outdoors from 20 m", to cover a horizontal area of 360° and a vertical area from -60° to 90°, whereby a mesh of approximately 44 million points per scan was generated.

A B C

A = Spatial distribution of trees and TLS device; B = Reflective target on a tree; C = Merged point cloud.

Figure 2. Spatial distribution, reflective target and point cloud.

Point clouds were merged with the FARO® SCENE Software version 5.5.3.16 (FARO, 2019), using 10 reflective targets placed before scanning (Figure 2B). The software aligned the point clouds using the geospatial information of the targets, to generate a single cloud (Figure 2C). The color unit of the scanner made it possible to visualize the pink labels, which made the identification of the trees easier.

Biomass calculation with the traditional method

The stem biomass was estimated using the diameter and height data, with allometric models developed for *Pinus cooperi*. We used the equation of Návar (2009), based solely on the *DBH* (Equation 1), and that of Vargas-Larreta et al. (2017), which incorporates height *h* (Equation 3). In addition, the generic models suggested by both authors for all pine species were considered (equations 2 and 4). Table 1 shows the expressions that were used.

Table 1. Allometric equations for *Pinus cooperi* C. E. Blanco and the *Pinus* L. genus.

Equation	ID	Author
$sW = 0.1899DBH^{2.2270}$	(1)	Návar (2009)
$sW = 0.0726DBH^{2.4459}$	(2)	
$sW = 0.0311DBH^{2.0936}h^{0.7688} + 0.0114DBH^{1.6760}h^{0.7463}$	(3)	Vargas-Larreta et al. (2017)
$sW = 0.0291DBH^{1.7417}h^{1.1661} + 0.0203DBH^{1.3330}h^{0.9289}$	(4)	

sW = Stem biomass (kg); *DBH* = Diameter at breast height (cm); *h* = Total height (m).

Estimation of TLS volume and biomass

The workflow included modeling the tree stem, calculating its volume, and estimating the biomass by multiplying the volume by the specific density value of *Pinus cooperi*. The entire process was based entirely on data derived from the point cloud. Statistical calculations and analysis, except for segmentation, were carried out in the R language version 4.4.1 (R Core Team, 2024) within the RStudio development software version 2023.12.1 Build 402 (RStudio Team, 2024). Only base functions and standard packages were used.

Data segmentation and normalization

The selected trees were individually segmented using the CloudCompare software version 2.13 (CloudCompare, 2024), removing branches and retaining only trunk points. The height of the stem was normalized by subtracting the minimum value of z, translating the base to z=0, and the total height was defined as the maximum value of z. To model the stem, it was divided into 5 cm intervals, and in each one the points were taken between ±2.5 cm, forming three-dimensional discs. Among these intervals, the interval corresponding to 1.30 meters from the ground containing the *DBH* was included. To reduce computational cost, the discs were projected in 2D by eliminating the z-coordinate and repeated points were discarded (Ye et al., 2020). Figure 3 shows the process described herein.

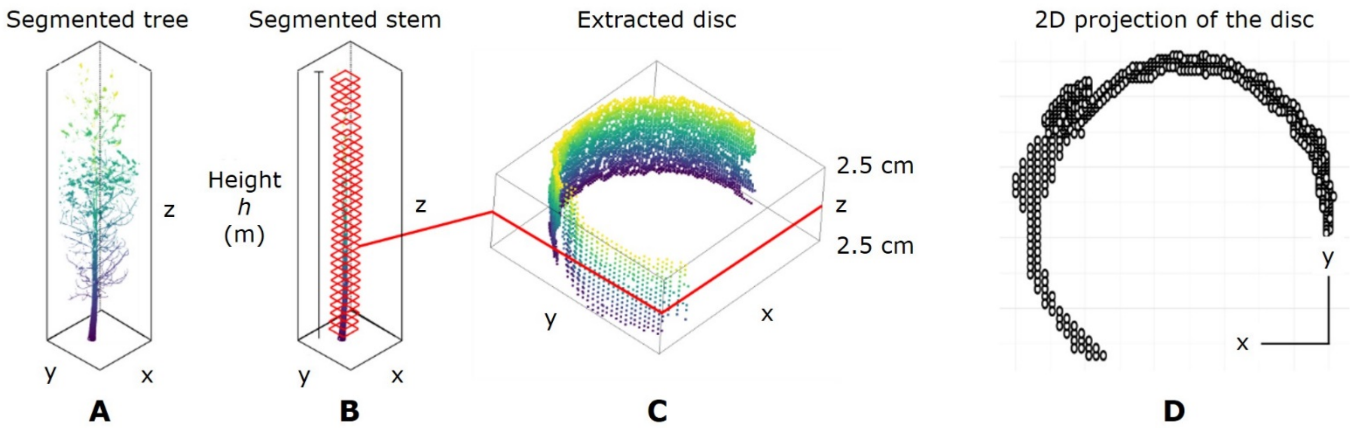

A = Segmented tree; B = Segmented stem; C = Example of disc extraction; D = Two-dimensional circumference.

Figure 3. Example of the disc extraction process at the individual tree level.

Estimation of the diameters in circumferences

The diameter of each projection was calculated by fitting a circumference to the points contained in its respective plane, defined by its center (h, k) and radius (*r*). This fit was approached as an optimization problem; the quadratic error between the points and the proposed circumference were minimized by means of the objective function of Umbach and Jones (2003) (Equation 5):

$$SS(h,k,r) = \sum_{i=1}^{n}\left(r - \sqrt{(x_i - h)^2 + (y_i - k)^2}\right)^2 \qquad (5)$$

Where:

SS = Sum of squared errors (m)

(h, k) = Center of the circumference

r = Radius of the circumference (m)

(x_i, y_i) = Point i of plane 2D

n = Number of points on the plane

Equation (5) was minimized, and the optimal values of h, k, and *r* were determined, with the Nelder-Mead method (Nelder & Mead, 1965), implemented through the "optim" function of the "stats" package. This approach, which requires few computational resources, employs the following initial parameters (equations 6 to 8) (Compeán-Aguirre et al., 2024).

$$h_0 = \bar{x} = \frac{1}{n}\sum_{i=1}^{n} x_i \qquad (6)$$

$$k_0 = \bar{y} = \frac{1}{n}\sum_{i=1}^{n} y_i \qquad (7)$$

$$r_0 = \frac{1}{n}\sum_{i=1}^{n} \sqrt{(x_i - h_0)^2 + (y_i - k_0)^2} \qquad (8)$$

Where:

h_0 = Average of x-coordinates

k_0 = Average of y-coordinates

r_0 = Average of the radius (m)

(x_i, y_i) = Point i of plane 2D

n = Number of points on the plane

Height-diameter ratio

The variation of the diameter of the stem along its height was modeled by the following Equation 9 (Kaitaniemi et al., 2020):

$$D_i = a{h_i}^{-b} \qquad (9)$$

Where:

D_i = Predicted diameter of segment i (m)

a, b = Statistical coefficients of the model

h_i = TLS height of the stem in segment i (m)

The model was fitted with the diameters previously calculated with the Nelder-Mead method (Nelder & Mead, 1965). The coefficients a and b were estimated with the "nls" function of the "stats" package; 70 % of the data were assigned to fit and 30 % to validate each model.

Volume and Biomass

The stem volume (sV) was calculated by integrating the cross-sectional area $A(h_i)$ from Equation 9. The radius of the segment i as a function of the height h_i is defined as:

$$r_i(h_i) = \frac{D_i(h_i)}{2} = \frac{a}{2} h_i^{-b} \qquad (10)$$

Where:

r_i = Predicted radius of segment i (m)

h_i = TLS height of the stem in segment i (m)

D_i = Predicted diameter of segment i (m)

a, b = Statistical coefficients of the model

Therefore, the cross-sectional area as a function of height is expressed as:

$$A(h_i) = \pi\, r_i(h_i)^2 = \pi \left(\frac{a}{2}\right)^2 h_i^{-2b} \qquad (11)$$

Where:

A = Cross-sectional area of segment i (m^2)

h_i = TLS height of the stem in segment i (m)

r_i = Predicted radius of segment i (m)

a, b = Statistical coefficients of the model

Integration of the cross-sectional area $A(h_i)$ from h_i=0 to h_i=h resulted in the equation of the volume of the stem as a function of height (Equation 12) and the values a and b (Equation 13):

$$sV = \frac{\pi a^2}{4} \int_0^h h_i^{-2b}\, dh_i \qquad (12)$$

$$sV(h, a, b) = \frac{\pi a^2}{4(-2b+1)} h^{-2b+1}, \text{ if } -2b + 1 > 0 \qquad (13)$$

Where:

sV = Stem volume (m^3)

a, b = Statistical coefficients of each model

h = Total TLS stem height (m)

h_i = TLS height of the stem in segment i (m)

dh_i = Differential of the variable *hi* (m)

Finally, the stem biomass was calculated by multiplying the total volume of each stem, obtained with Equation (13), by the density of the wood, as indicated in the following expression:

$$sW = sV \times \rho \qquad (14)$$

Where:

sW = Stem biomass (kg)

sV =Stem volume (m^3)

ρ = 416 kg m^3. Value cited by Silva-Arredondo and Návar-Cháidez (2012) for *Pinus cooperi*.

Statistical analysis and assessment metrics

The normality of the data for diameter (*DBH*), height (*h*), and biomass (*sW*) was evaluated with the Shapiro-Wilk test, using both the values of the traditional instruments and the TLS. The diameter and height followed a normal distribution with both methods. After assessing the homogeneity of the variances with Levene's test, their means were compared using Student's *t*-test with 95 % confidence. For biomass, being non-normal, the Kruskal-Wallis test and a Dunn's *post hoc* analysis with Bonferroni correction (Haynes, 2013), using the dunn.test package version 1.3.6 (Dinno, 2024) and a confidence interval of 95 % were applied. In addition, the *RMSE* (Equation 15) and R^2 (Equation 16) were calculated for diameter and height. The observed values of *DBH* and height were assumed to correspond to caliper and hypsometer measurements, and predicted values were estimated with TLS.

$$RMSE = \sqrt{\frac{1}{n}\sum_{i=1}^{n}(y_i - \hat{y}_i)^2} \qquad (15)$$

$$R^2 = \frac{\sum_{i=1}^{n}(y_i-\hat{y}_i)^2}{\sum_{i=1}^{n}(y_i-\bar{y})^2} \qquad (16)$$

Where:

RMSE = Root mean squared error

R^2 = Coefficient of determination

y_i = Observed values

$\hat{y}_i$ = Predicted values

$\bar{y}$ = Average of the observed values

n = Total number of observations

Results and Discussion

The analysis of the variable *h* obtained with the hypsometer and the TLS point cloud estimated a mean of 12.29 m and 10.82 m, respectively (Table 2). The Shapiro-Wilk test confirmed the normality of the data in both methods (p=0.1168 and p=0.9113), and Levene's test indicated homogeneity of variances (p=0.1569). Under these assumptions, Student's *t*-test showed significant differences between both methods (t=-4.1464, p=0.0001). This is confirmed by Figure 4A. The *RMSE* of the TLS, with respect to the hypsometer is 1.68 m, with a R^2 of 0.79, as shown in the scatter plot in Figure 4B.

Table 2. Descriptive statistics of *h* obtained in both methods.

	***h* (m) *n*=31**			
Method	**Minimum**	**Mean**	**Maximum**	***SD***
Hypsometer	8.80	12.29	17.60	1.64
TLS	8.59	10.82	13.29	1.10

h = Height; *n* = Total number of observations; *SD* = Standard deviation.

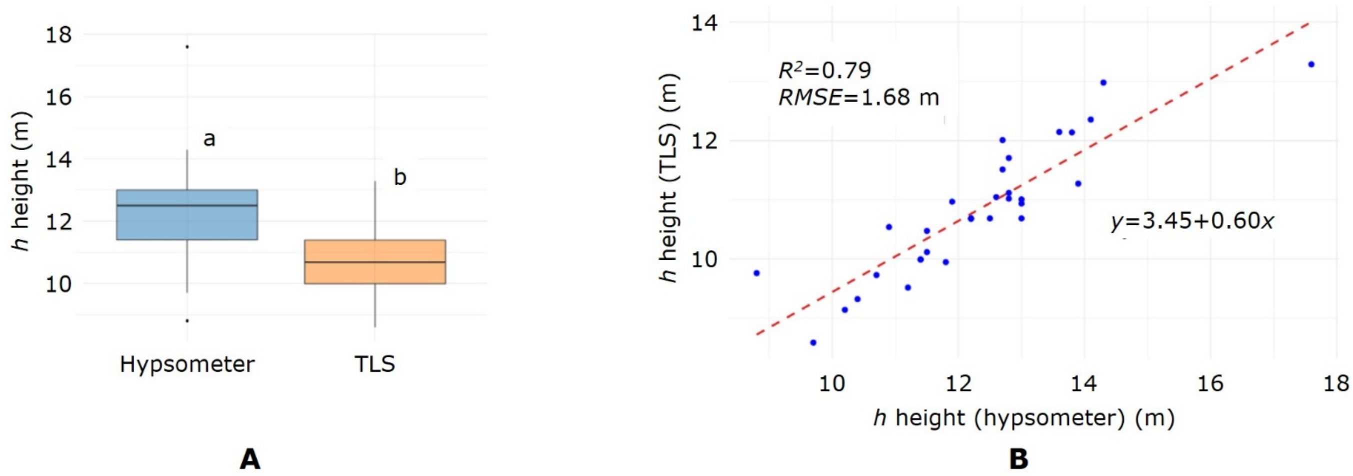

A = Comparison of the variable *h* in the different methods; B = Scatter plot and line of adjustment for variable *h*.

Figure 4. Analysis of the height *h* measured with the hypsometer *versus* the TLS.

It is important to consider that the actual height of the trees is an unknown parameter, so any comparison should be interpreted with caution. Although the TLS offers greater accuracy than the hypsometer and is free from the error associated with manual measurement, occlusions in the data capture can affect the estimation of the height. The results are consistent with Liu et al. (2018), who documented an average *RMSE* of 0.95 m in height measurements with TLS, they highlighted biases related to canopy density and terrain obstructions. De Petris et al. (2022) noted that terrain slope affects the accuracy of the measurements, while hypsometers are more prone to angular errors at distances of less than 20 m; TLS systems may face problems of specular reflection and signal attenuation at greater distances (Tan et al., 2018). These instrumental limitations and site conditions would contribute substantially to the increased *RMSE* of the study.

Regarding the *DBH*, no significant differences were obtained between the assessed methods: it was 15.92 cm on average when measured with the caliper, and 15.73 cm when TLS was utilized (Table 3). The Shapiro-Wilk test confirmed the normality of the data (p=0.6292 and p=0.2032), and Levene's test indicated homogeneity of the variances (p=0.8005). Student's t-test exhibited no significant difference between methods (t=0.3295, p=0.7429). Figure 5A shows the comparison between means. The difference in the *RMSE* between the caliper and TLS was 1.28 cm, with an R^2=0.72 (Figure 5B).

Table 3. Statistic describing the *DBH* in both methods.

	***DBH* (cm)** ***n*=31**			
Method	**Minimum**	**Mean**	**Maximum**	***SD***
Caliper	12.35	15.92	20.32	2.20
TLS	11.33	15.73	21.79	2.39

DBH = Diameter at breast height; *n* = Total number of observations; *SD* = Standard deviation.

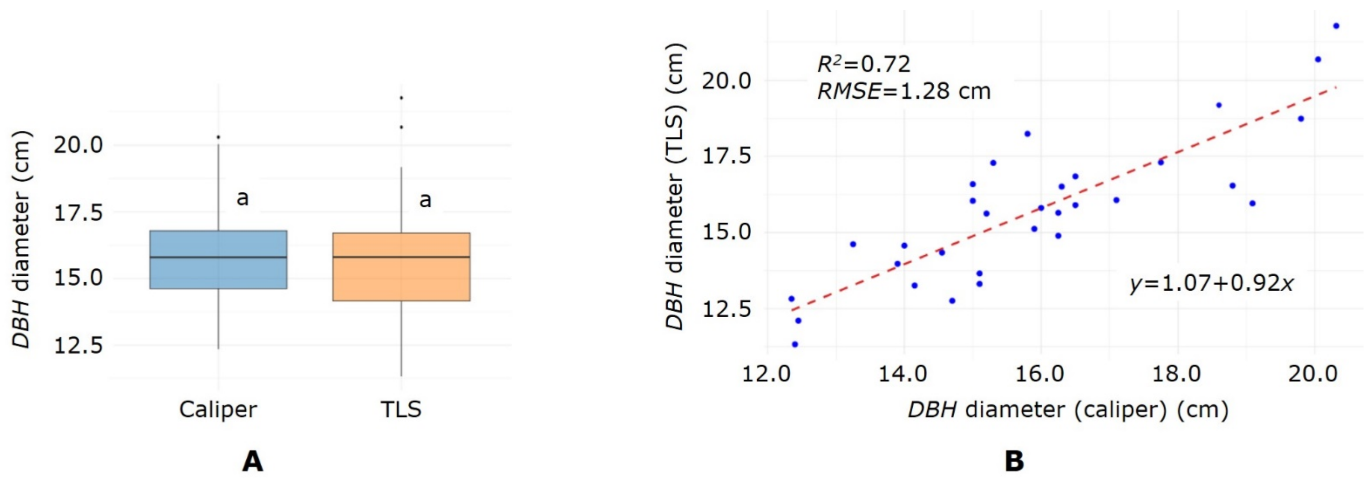

A = *DBH* comparison between the various methods; B = Scatter plot and fit line for the *DBH*.

Figure 5. Analysis of the variable *DBH* measured with the caliper *versus* TLS.

These results are lower than those reported by Wu et al. (2024), who obtained an *RMSE* of 5.26 cm in tropical forests, with trees of complex morphologies. However, they are larger than those of Pitkänen et al. (2019), who estimated an *RMSE* of 0.73 cm using cylindrical instead of two-dimensional processing. Three-dimensional fitting, although more accurate, has a higher computational cost (Ye et al., 2020). The fitted models for the TLS height/diameter ratio showed a high capacity to describe the diameter variation along the stem, with an average R^2 of 0.91 and a *RMSE* of 0.50 cm, calculated with the validation data (30 %). Table 4 shows the descriptive statistics of the evaluation metrics and coefficients a and b. While the consistency of these parameters highlights the applicability of the model for the digital reconstruction of the stem, the underestimation of the height introduces a bias that will affect any calculation. Figure 6A shows the reconstructed stem of a tree. It is important to mention that the applied model does not consider the curvature of the trunk; likely, this factor will also have an impact on subsequent calculations. Figure 6B shows the variation of the diameter in the first two meters and the response curve of the model generated for a single tree.

Table 4. Descriptive statistics of the height-diameter model (Equation 9).

***n*=31**				
Parameter	**Minimum**	**Mean**	**Maximum**	***SD***
R^2	0.68	0.92	1.00	0.07
RMSE (cm)	0.13	0.50	1.13	0.25
a	0.11	0.15	0.22	0.02
b	0.04	0.09	0.16	0.03

n = Total number of observations; R^2 = Coefficient of determination; *RMSE* = Root mean squared error; a, b = Coefficients; *SD* = Standard deviation.

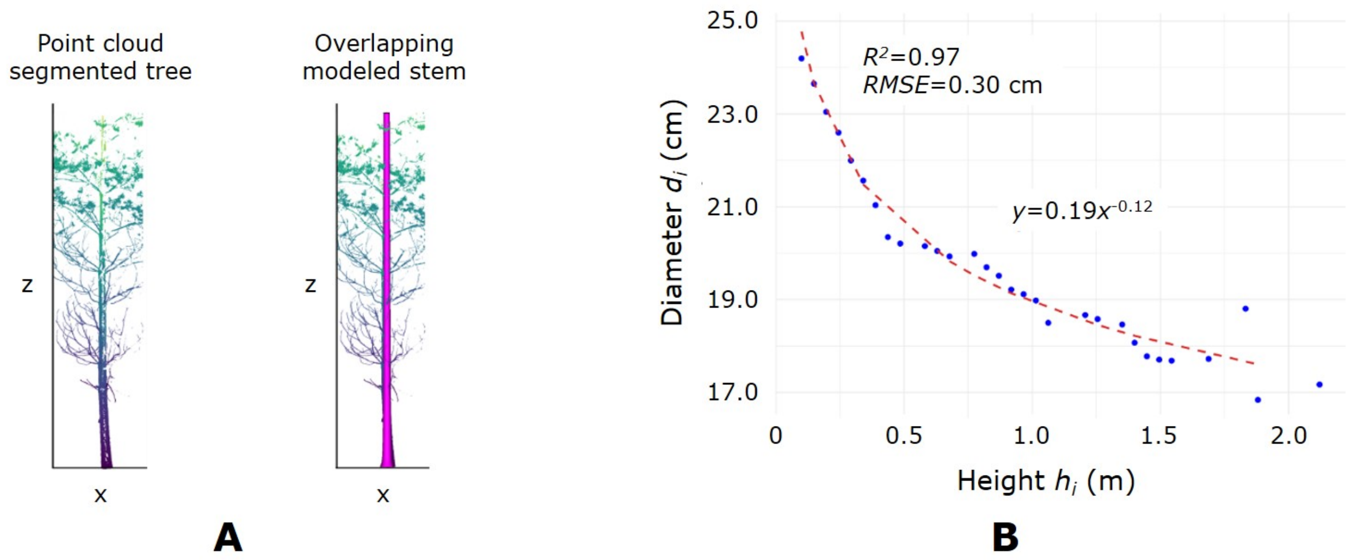

A = Estimated stem of the point cloud; B = Scatter plot of *DBH-h* variation.

Figure 6. Example of a reconstructed stem and its model response curve.

Table 5 summarizes the descriptive statistics of the volumes calculated for the 31 stems, with an average value of 0.17 m^3. The variability of the volume between trees is due to differences in diameters and heights. Underestimation of the height due to TLS limitations (Tan et al., 2018) is a source of error, especially in tall trees or trees with occlusions in point clouds.

Table 5. Descriptive statistics of the estimated volume.

***n*=31**				
Variable	**Minimum**	**Mean**	**Maximum**	***SD***
sV (m^3)	0.07	0.17	0.36	0.01

n = Total number of observations; *sV* = Stem volume; *SD* = Standard deviation.

The mean biomass estimated with TLS was 68.78 kg, with a tendency to underestimate the values compared to the traditional allometric methods (Table 6) due to the underestimation of the height. Finally, the analysis indicated that the biomass data do not follow a normal distribution, according to the Shapiro-Wilk test ($p<0.05$). The Kruskal-Wallis nonparametric test confirmed significant differences between the methods evaluated ($X^2=20.18$, $p=0.001$). Dunn's *post hoc* analysis, with Bonferroni correction, revealed that the biomass estimates using TLS differed significantly from those obtained with Equation 1 ($p=0.0015$), but not with the other methods ($p>0.05$). According to this analysis, the TLS and Equation 2 belong to group "a"; both Equation 3 and 4 are in an intermediate position, within group "ab" (Figure 7). Although the results point to the TLS estimating biomass within the expected ranges, they are not conclusive, as other factors such as the error cited by Návar (2009) and the cumulative error present in the equations of Vargas-Larreta et al. (2017) should be considered.

Table 6. Descriptive statistics of the estimated biomass.

Method	**Stem biomass *sW* (kg) *n*=31**				
	Minimum	**Median**	**Mean**	**Maximum**	***SD***
Equation 1[b]	51.25	88.70	92.47	155.25	28.83
Equation 2[a]	33.97	62.05	65.27	114.74	22.40
Equation 3[ab]	40.82	77.28	80.82	169.45	29.95
Equation 4[ab]	40.33	74.75	78.24	172.47	28.77
TLS[a]	31.61	63.35	68.78	149.95	28.38

n = Total number of observations; [a, b] Different letters indicate significant statistical differences; *SD* = Standard deviation.

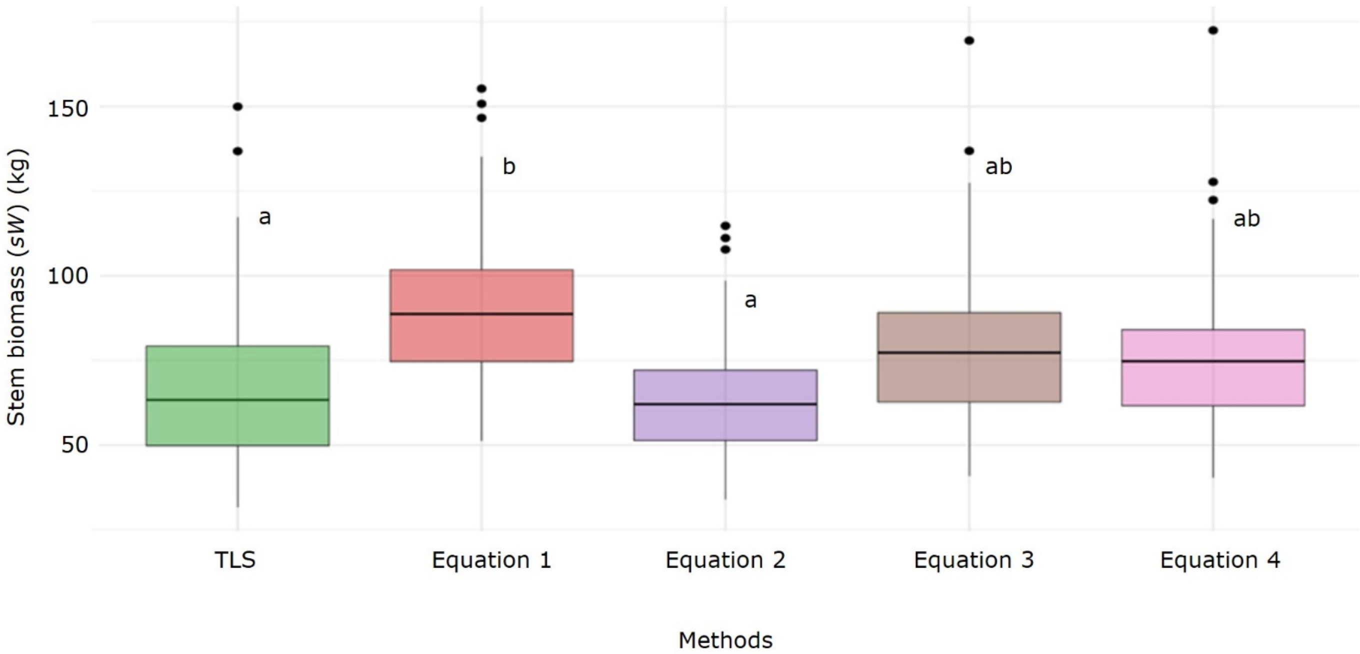

Figure 7. Box-and-whisker plot of biomass values for each method.

The main issue in the present study was the underestimation of the height (*h*) obtained by TLS, which affects the calculation of the stem biomass. This finding is in agreement with Cabo et al. (2018) and Wang et al. (2023), who mention that structural occlusions and information loss in the upper parts of the tree are common limitations of TLS, especially in tall and dense trees. Kükenbrink et al. (2021) also observed underestimates in complex structures, despite the high accuracy of the TLS (R^2=0.954) in urban trees. On the other hand, the results contrast with Krause et al. (2023), who indicate that total aboveground biomass estimates using TLS are, on average, 10 % higher than those obtained with allometric equations. This discrepancy could be explained by the fact that their paper includes both the trunk and the main branches, while this study focuses exclusively on the stem.

The proposed methodology proves efficient in computational resources and offers acceptable results, but has limitations such as the use of a fixed density value for *Pinus cooperi* and the study of a single species with a limited sample. In addition, manual dot removal is time-consuming. Although the costs and timing are not addressed, the implementation of TLS requires a high investment in the sensor, infrastructure, and trained personnel, which could be a challenge in Mexico. It is also important to mention that the variability of ecosystems and equipment makes it difficult to compare methodologies. Future research could focus on automating segmentation, exploring the use of dynamic density values, and studying different ecosystems. Also, it would be relevant to integrate information from other sources, such as satellite images.

Conclusions

The TLS showed high accuracy in the estimation of *DBH* (R^2=0.72; *RMSE*=1.28 cm) when considering the measurements of the caliper as reference. As for the estimation of the total height (R^2=0.79; *RMSE*=1.68 m), special caution should be taken when using this method, since the crown density significantly influences the results. The present methodology allows estimating the aboveground biomass at the individual tree level with acceptable accuracy; however, its practical application should be considered with reservations, as site conditions and traditional methodologies used may influence the accuracy of the measurements. It is recommended, in future research, to incorporate complementary technologies such as aerial LiDAR scanners to improve the accuracy of height estimation, as well as to include additional variables such as stem curvature. In addition, it is necessary to develop algorithms for the detection and segmentation of trees with TLS data to cover large areas in the shortest possible time, to extend the analysis to different tree species, and to generate specific allometric equations based on TLS data.

Acknowledgments

The authors thank the National Council for Humanities, Science, and Technology (*Consejo Nacional de Humanidades*, *Ciencias y Tecnologías*, *Conahcyt*) for the scholarship granted for the doctoral program, and the Council for Science and Technology of the State of *Durango* (*Consejo de Ciencia y Tecnología del Estado de Durango*, *Cocyte*d) for its support.

Conflict of interest

The authors declare that they have no conflict of interest.

Contribution by author

Jorge Luis Compeán-Aguirre: statistical analysis, drafting of the manuscript, methodology; Pablito Marcelo López-Serrano and José Luis Silván-Cárdenas: methodology, revision and editing of the manuscript; Ciro Andrés Martínez-García-Moreno and Daniel José Vega-Nieva: revision and coordination of the revision process; José Javier Corral-Rivas: field sampling and revision of the manuscript.

References

Ashraf, M. I., Zhao, Z., Bourque, C. P.-A., MacLean, D. A., & Meng, F.-R. (2013). Integrating biophysical controls in forest growth and yield predictions with artificial intelligence technology. *Canadian Journal of Forest Research*, *43*(12), 1162-1171. https://doi.org/10.1139/cjfr-2013-0090

Bhandari, S. K., & Nandy, S. (2024). Forest aboveground biomass prediction by integrating terrestrial laser scanning data, Landsat 8 OLI-derived forest canopy density and spectral indices. *Journal of the Indian Society of Remote Sensing*, *52*, 813-824. https://doi.org/10.1007/s12524-023-01687-z

Bornand, A., Rehush, N., Morsdorf, F., Thürig, E., & Abegg, M. (2023). Individual tree volume estimation with terrestrial laser scanning: Evaluating reconstructive and allometric approaches. *Agricultural and Forest Meteorology*, *341*, Article 109654. https://doi.org/10.1016/j.agrformet.2023.109654

Borsah, A. A., Nazeer, M., & Wong, M. S. (2023). LIDAR-based forest biomass remote sensing: A review of metrics, methods, and assessment criteria for the selection of allometric equations. *Forests*, *14*(10), 2095. https://doi.org/10.3390/f14102095

Cabo, C., Ordóñez, C., López-Sánchez, C. A., & Armesto, J. (2018). Automatic dendrometry: Tree detection, tree height and diameter estimation using terrestrial laser scanning. *International Journal of Applied Earth Observation and Geoinformation*, *69*, 164-174. https://doi.org/10.1016/j.jag.2018.01.011

Calders, K., Newnham, G., Burt, A., Murphy, S., Raumonen, P., Herold, M., Culvenor, D., Avitabile, V., Disney, M., Armston, J., & Kaasalainen, M. (2015). Nondestructive estimates of above-ground biomass using terrestrial laser scanning. *Methods in Ecology and Evolution*, *6*(2), 198-208. https://doi.org/10.1111/2041-210X.12301

Chojnacky, D. C., Heath, L. S., & Jenkins, J. C. (2014). Updated generalized biomass equations for North American tree species. *Forestry: An International Journal of Forest Research*, *87*(1), 129-151. https://doi.org/10.1093/forestry/cpt053

CloudCompare. (2024). *CloudCompare project* (version 2.13) [Software]. CloudCompare. https://www.cloudcompare.org/

Compeán-Aguirre, J. L., & López-Serrano, P. M. (2024). Bibliometric insights into terrestrial laser scanning for forest biomass estimation. *Ecologies*, *5*(3), 470-490. https://doi.org/10.3390/ecologies5030029

Compeán-Aguirre, J. L., López-Serrano, P. M., Silván-Cárdenas, J. L., Martínez-García-Moreno, C. A., Vega-Nieva, D. J., Corral-Rivas, J. J., & Pompa-García, M. (2024). Evaluation of two-dimensional DBH estimation algorithms using TLS. *Forests*, *15*(11), 1964. https://doi.org/10.3390/f15111964

De Petris, S., Sarvia, F., & Borgogno-Mondino, E. (2022). About tree height measurement: Theoretical and practical issues for uncertainty quantification and mapping. *Forests*, *13*(7), 969. https://doi.org/10.3390/f13070969

Dinno, A. (2024). *dunn.test: Dunn's test of multiple comparisons using rank sums* (version 1.3.6) [Software]. CRAN. https://doi.org/10.32614/CRAN.package.dunn.test

Disney, M. I., Vicari, M. B., Burt, A., Calders, K., Lewis, S. L., Raumonen, P., & Wilkes, P. (2018). Weighing trees with lasers: Advances, challenges and opportunities. *Interface Focus*, *8*, Article 20170048. https://doi.org/10.1098/rsfs.2017.0048

FARO. (2019). *FARO® SCENE Software* (versión 5.5.3.16) [Software]. FARO. https://www.faro.com/es-MX/Products/Software/SCENE-Software

Galeote-Leyva, B., Valdez-Lazalde, J. R., Ángeles-Pérez, G., de los Santos-Posadas, H. M., y Romero-Padilla, J. M. (2022). Inventario forestal asistido por LIDAR: efecto de la densidad de retornos y el diseño de muestreo sobre la precisión. *Madera y Bosques*, 28(2), Artículo e2822330. https://doi.org/10.21829/myb.2022.2822330

García, E. (2004). *Modificaciones al sistema de clasificación climática de Köppen*. Instituto de Geografía de la Universidad Nacional Autónoma de México. https://publicaciones.geografia.unam.mx/index.php/ig/catalog/book/83

Haynes, W. (2013). Bonferroni correction. In W. Dubitzky, O. Wolkenhauer, K.-H. Cho & H. Yokota (Eds.), *Encyclopedia of Systems Biology* (p. 154). Springer. https://doi.org/10.1007/978-1-4419-9863-7_1213

Hernández-Moreno, J. A., Pérez-Salicrup, D. R., y Velázquez-Martínez, A. (2025a). Medición de parámetros de inventario forestal en bosques plantados mediante tecnología *LiDAR*: Comparación de métodos. *Revista Mexicana de Ciencias Forestales*, *16*(87), 72-99. https://doi.org/10.29298/rmcf.v16i87.1488

Hernández-Moreno, J. A., Velázquez-Martínez, A., Pérez-Salicrup, D. R., Bravo, F., MacFarlane, D. W., & Reyes-Hernández, V. J. (2025b). Terrestrial laser scanning for estimating the volume and biomass of coniferous stems in the Mariposa Monarca Biosphere Reserve, Mexico. *Forests*, *16*(2), 334. https://doi.org/10.3390/f16020334

Hoover, C. M., & Smith, J. E. (2020). *Selecting a minimum diameter for forest biomass and carbon estimation: How low should you go?* (General Technical Report NRS-196). United States Department of Agriculture, Forest Service. https://www.fs.usda.gov/nrs/pubs/gtr/gtr_nrs196.pdf

Hummel, F. C., Locke, G. M. L., Jeffers, J. N. R., & Christie, J. M. (1959). *Code of sample plot procedure* (Forestry Commission Bulletin No. 31). Forestry Commission. https://cdn.forestresearch.gov.uk/1959/04/fcbu031.pdf

Huy, B., Kralicek, K., Poudel, K. P., Phuong, V. T., Khoa, P. V., Hung, N. D., & Temesgen, H. (2016). Allometric equations for estimating tree aboveground biomass in evergreen broadleaf forests of Viet Nam. *Forest Ecology and Management*, 382, 193-205. https://doi.org/10.1016/j.foreco.2016.10.021

Islas-Gutiérrez, F., Cruz-Juárez, E., Buendía-Rodríguez, E., Guerra-De la Cruz, V., Pineda-Ojeda, T., Flores-Ayala, E., Carrillo-Anzures, F., y Acosta-Mireles, M. (2024). Ecuación alométrica para estimar biomasa aérea de árboles de *Pinus hartwegii* Lindl. a partir de datos LiDAR. *Revista Fitotecnia Mexicana*, *47*(1), 70-79. https://doi.org/10.35196/rfm.2024.1.70

Kaitaniemi, P., Lintunen, A., & Sievänen, R. (2020). Power-law estimation of branch growth. *Ecological Modelling*, *416*, Article 108900. https://doi.org/10.1016/j.ecolmodel.2019.108900

Kankare, V., Holopainen, M., Vastaranta, M., Puttonen, E., Yu, X., Hyyppä, J., Vaaja, M., Hyyppä, H., & Alho, P. (2013). Individual tree biomass estimation using terrestrial laser scanning. *ISPRS Journal of Photogrammetry and Remote Sensing*, *75*, 64-75. https://doi.org/10.1016/j.isprsjprs.2012.10.003

Krause, P., Forbes, B., Barajas-Ritchie, A., Clark, M., Disney, M., Wilkes, P., & Bentley, L. P. (2023). Using terrestrial laser scanning to evaluate non-destructive aboveground biomass allometries in diverse Northern California forests. *Frontiers in Remote Sensing*, *4*, Article 1132208. https://doi.org/10.3389/frsen.2023.1132208

Kükenbrink, D., Gardi, O., Morsdorf, F., Thürig, E., Schellenberger, A., & Mathys, L. (2021). Above-ground biomass references for urban trees from terrestrial laser scanning data. *Annals of Botany*, *128*(6), 709-724. https://doi.org/10.1093/aob/mcab002

Liang, X., Hyyppä, J., Kaartinen, H., Lehtomäki, M., Pyörälä, J., Pfeifer, N., Holopainen, M., Brolly, G., Francesco, P., Hackenberg, J., Huang, H., Jo, H.-W., Katoh, M., Liu, L., Mokroš, M., Morel, J., Olofsson, K., Poveda-Lopez, J., Trochta, J., ... Wang, Y. (2018). International benchmarking of terrestrial laser scanning approaches for forest inventories. *ISPRS Journal of Photogrammetry and Remote Sensing*, *144*, 137-179. https://doi.org/10.1016/j.isprsjprs.2018.06.021

Liu, G., Wang, J., Dong, P., Chen, Y., & Liu, Z. (2018). Estimating individual tree height and Diameter at Breast Height (DBH) from Terrestrial Laser Scanning (TLS) data at plot level. *Forests*, *9*(7), 398. https://doi.org/10.3390/f9070398

Montoya, O., Icasio-Hernández, O., & Salas, J. (2021). TreeTool: A tool for detecting trees and estimating their DBH using forest point clouds. *SoftwareX*, *16*, Article 100889. https://doi.org/10.1016/j.softx.2021.100889

Návar, J. (2009). Allometric equations for tree species and carbon stocks for forests of Northwestern Mexico. *Forest Ecology and Management*, *257*(2), 427-434. https://doi.org/10.1016/j.foreco.2008.09.028

Nelder, J. A., & Mead, R. (1965). A simplex method for function minimization. *The Computer Journal*, *7*(4), 308-313. https://doi.org/10.1093/comjnl/7.4.308

Ortiz-Reyes, A. D., Valdez-Lazalde, J. R., Ángeles-Pérez, G., De los Santos-Posadas, H. M., Schneider, L., Aguirre-Salado, C. A., y Peduzzi, A. (2019). Transectos de datos LiDAR: una estrategia de muestreo para estimar biomasa aérea en áreas forestales. *Madera y Bosques*, *25*(3), Artículo e2531872. https://doi.org/10.21829/myb.2019.2531872

Ortiz-Reyes, A. D., Velasco-Bautista, E., Correa-Díaz, A., y Ángeles-Pérez, G. (2022). Predicción de variables dasométricas mediante modelos lineales mixtos y datos de LiDAR aerotransportado. *e-CUCBA*, *9*(17), 88-95. https://www.researchgate.net/publication/360011682_Prediccion_de_variables_dasometricas_mediante_modelos_lineales_mixtos_y_datos_de_LiDAR_aerotransportado

Pitkänen, T. P., Raumonen, P., & Kangas, A. (2019). Measuring stem diameters with TLS in boreal forests by complementary fitting procedure. *ISPRS Journal of Photogrammetry and Remote Sensing*, *147*, 294-306. https://doi.org/10.1016/j.isprsjprs.2018.11.027

R Core Team. (2024). *R: A Language and Environment for Statistical Computing* (version 4.4.1) [Software]. R Foundation for Statistical Computing. https://www.R-project.org/

RStudio Team. (2024). *RStudio* (version 2023.12.1 Build 402) [Software]. Posit Software. https://posit.co/products/open-source/rstudio/

Segura, M., y Andrade, H. J. (2008). ¿Cómo construir modelos alométricos de volumen, biomasa o carbono de especies leñosas perennes? *Agroforestería en las Américas*, *46*, 89-96. https://repositorio.catie.ac.cr/handle/11554/6935

Silva-Arredondo, F. M., y Návar-Cháidez, J. de J. (2012). Estimación de la densidad de madera en árboles de comunidades forestales templadas del norte del estado de Durango, México. *Madera y Bosques*, *18*(1), 77-88. https://doi.org/10.21829/myb.2012.1811139

Tan, K., Zhang, W., Shen, F., & Cheng, X. (2018). Investigation of TLS intensity data and distance measurement errors from target specular reflections. *Remote Sensing*, *10*(7), 1077. https://doi.org/10.3390/rs10071077

Umbach, D., & Jones, K. N. (2003). A few methods for fitting circles to data. *IEEE Transactions on Instrumentation and Measurement*, *52*(6), 1881-1885. https://doi.org/10.1109/TIM.2003.820472

Vargas-Larreta, B., López-Sánchez, C. A., Corral-Rivas, J. J., López-Martínez, J. O., Aguirre-Calderón, C. G., & Álvarez-González, J. G. (2017). Allometric equations for estimating biomass and carbon stocks in the temperate forests of North-Western Mexico. *Forests*, *8*(8), 269. https://doi.org/10.3390/f8080269

Wang, F., Sun, Y., Jia, W., Zhu, W., Li, D., Zhang, X., Tang, Y., & Guo, H. (2023). Development of estimation models for individual tree aboveground biomass based on TLS-derived parameters. *Forests*, *14*(2), 351. https://doi.org/10.3390/f14020351

Wu, Y., Gan, X., Zhou, Y., & Yuan, X. (2024). Estimation of Diameter at Breast Height in tropical forests based on Terrestrial Laser Scanning and shape diameter function. *Sustainability*, *16*(6), 2275. https://doi.org/10.3390/su16062275

Ye, W. F., Qian, C., Tang, J., Liu, H., Fan, X. Y., Liang, X., & Zhang, H. J. (2020). Improved 3D stem mapping method and elliptic hypothesis-based DBH estimation from terrestrial laser scanning data. *Remote Sensing*, *12*(3), 352. https://doi.org/10.3390/rs12030352